Machine Learning and Artificial Intelligence
J.-L. Kim (Ed.)

doi:10.3233/FAIA220427

Generalized Multiquadric Neural Networks in Image Reconstruction

Pornthip PONGCHALEE[a], Pirapong INTHAPONG[b], Krittidej CHANTHAWARA[c], Pichapop PAEWPOLSONG[b], and Sayan KAENNAKHAM[b,1]
[a] *Department of Applied Mathematics and Statistics, Faculty of Science and Liberal Arts, Rajamangala University of Technology Isan, Nakhon Ratchasima 30000, Thailand.*
[b] *School of Mathematics, Institute of Science, Suranaree University of Technology, Nakhon Ratchasima, 30000, Thailand.*
[c] *Program of Mathematics, Faculty of Science, Ubon Ratchathani Rajabhat University, Ubon Ratchathani 34000, Thailand.*

Abstract. This work aims to numerically investigate the performance of the multiquadric (MQ) radial basis function in more general formats for image reconstruction applications. Desired features, i.e., accuracy and shape parameter sensitivity, of each form is numerically compared and explored. The famous Lena image is damaged using two levels of damage: 20% and 40%, in a Salt-and-Pepper manner. It has been discovered in this work that $\beta = 3/2$ produces reasonably good accuracy and is least affected by the change in shape parameter while keeping both the CPU time and the condition number reasonably acceptable. This finding is promising and useful for further applications of MQ in more complex contexts.

Keywords. Generalized multiquadric, neural networks, image reconstruction

1. Introduction

Radial basis functions or RBFs have been receiving a great amount of interest ever since they were introduced in 1971. This also includes the advantages for solving partial differential equations known as 'meshfree or meshless' methods [1-3]. The multivariate property has made RBF attractive in a wide range of applications and one of the most popular RBF choices is the so-called multiquadric (MQ-RBF). The original and non-normalized formula under this type of RBFs is $\left(\varepsilon^2 + r^2\right)^{\beta}$ with ε being the so-called 'shape parameter' and $r = \left\| \mathbf{x} - \mathbf{x}^{\Theta} \right\|_2$ for $\mathbf{x}, \mathbf{x}^{\Theta} \in \mathbb{R}^n$ represents the distance function. Ever since it was implemented numerically, only $\beta = -1/2$ and $\beta = -1/2$ have been receiving attention where the solutions are known to be highly dependent on ε, [4-7]. This challenge has come to our attention as whether there is a β that is less affected by the choice of ε. The study in this path is named as 'Generalized MQ or GMQ) and was

[1] Corresponding Author, Sayan KAENNAKHAM, School of Mathematics, Institute of Science, Suranaree University of Technology, Nakhon Ratchasima, 30000, Thailand. E-mail: sayan_kk@g.sut.ac.th.

firstly approached by Maggie E. Chenoweth [8] in 2009. Over the years, not much numerical work has been done until one of our preliminary works done in 2021 [9].

The focus of this work is paid to the numerical application of GMQ under the context of image reconstruction investigated under the structure of a neural network (with space limitation, more details are found in [9]). For this, ten forms of GMQ were numerically investigated and their performances were monitored and recorded.

2. Mathematical methodology

2.1. Interpolation with RBFNs

The investigation begins with the study of a multivariate function $g:\Xi\to\mathbb{R}$, where $\Xi\subset\mathbb{R}^m$, from a set of sample values $\left\{g\left(\mathbf{x}_j\right)\right\}_{j=1}^{M}$ on a discrete set $\mathrm{X}=\left\{\mathbf{x}_j\right\}_{j=1}^{M}\subset\Xi$ (later referred to as 'centres'). Such multivariate functions can be efficiently reconstructed if they are approximated by linear combinations of univariate interpolation functions with the Euclidean norm $\|\cdot\|_2$. In the mathematical literature, ϕ is often called a radial basis function with centres $\left\{\mathbf{x}_j\right\}_{j=1}^{M}$ and Θ is the associated kernel. Interpolants G of g can be constructed as $G(\mathbf{x})=\sum_{j=1}^{M}a_j\phi\left(\left\|\mathbf{x}-\mathbf{x}_j\right\|_2\right)$ with real coefficients, $\left\{a_j\right\}_{j=1}^{M}$ which is determined using the interpolating condition $G(\mathbf{x}_i)=g(\mathbf{x}_i),$ for all $i=1, 2, ..., M$, and it yields.

$$g(\boldsymbol{x}_i)=G(\boldsymbol{x}_i)=\sum_{j=1}^{M}a_j\phi\left(\left\|\boldsymbol{x}_i-\boldsymbol{x}_j\right\|_2\right) \tag{1}$$

Hence, what comes next is a system of linear equations with $\left\{a_j\right\}_{j=1}^{M}$ being the unknowns, expressed as $\boldsymbol{\Phi}\boldsymbol{\alpha}=\mathbf{g}$, where $\boldsymbol{\alpha}=\left[a_1,\ldots,a_M\right]^T$ and $\mathbf{g}=\left[g\left(\mathbf{x}_1\right),\ldots,g\left(\mathbf{x}_M\right)\right]^T$, and $\boldsymbol{\Phi}=\left[\phi_{ij}\right]_{M\times M}$ is the symmetric $M\times M$ matrix. Once the coefficient matrix, $\boldsymbol{\alpha}$, is obtained, the solution calculation process can then proceed. For unknown locations $\hat{\mathrm{X}}=\left\{\hat{\mathbf{x}}_j\right\}_{j=1}^{\hat{M}}\subset\Xi$ and $\mathrm{X}\cap\hat{\mathrm{X}}=\phi$, the approximate values of the corresponding function $\hat{g}\left(\hat{\boldsymbol{x}}_j\right)$is obtained for all $j=1,2,...,\hat{M}$, by.

$$\hat{g}\left(\hat{\boldsymbol{x}}_j\right)\approx G(\hat{\boldsymbol{x}}_j)=\sum_{i=1}^{M}a_j\phi\left(\left\|\hat{\boldsymbol{x}}_j-\boldsymbol{x}_i\right\|_{2},\varepsilon\right) \tag{2}$$

2.2. Generalized Multiquadric (GMQ)

The multiquadric (MQ) basis function, in its generalized form, which is defined as follows, is the main focus of this paper.

$$\phi_j(\boldsymbol{x}) = \left(\varepsilon^2 + r_j{}^2\right)^{\beta} = \left(\varepsilon^2 + \left\|\boldsymbol{x} - \boldsymbol{x}_j\right\|^2\right)^{\beta} \tag{3}$$

where $\beta = \ldots, -3/2, -1/2, 1/2, 3/2, \ldots$. These values produce different curves (see Figure 1.) and have a direct bearing on the solvability of matrix involved.

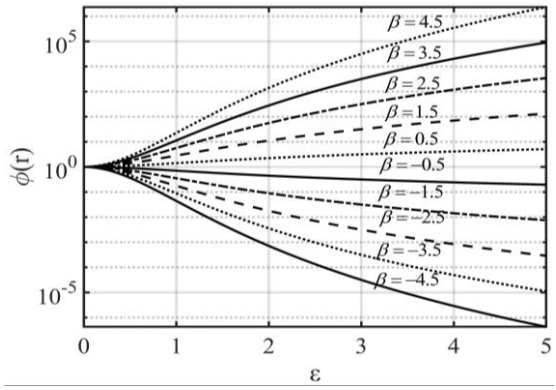

Figure 1. Function profiles of GMQ for each value of β'*s* (plotted only on the positive half of *x*-axis).

3. Numerical algorithm

Step 1. Two groups of pixels are created; the set of corrupted pixels ($\hat{\Omega}$, containing $\hat{M}$ elements), and the rest (Ω , containing M elements).

Step 2. For each $\mathbf{x}_i = (x_i, y_i) \in \Omega$, $i = 1, 2, ..., M$, and choose $m = 3$.

2.1 Choose β for GMQ and Construct the interpolation matrix $\left[\boldsymbol{\Phi}\right]_{(M+3)\times(M+3)}$.

2.2 Solve $\left[\boldsymbol{\Phi}\right]_{(M+3)\times(M+3)}\left[\mathbf{A}\right]_{(M+3)\times(1)} = \left[\mathbf{G}\right]_{(M+3)\times(1)}$, to get the coefficient matrix $\mathbf{A}$.

Step 3. For each $\hat{\mathbf{x}}_j = (x_j, y_j) \in \hat{\Omega}$, $j = 1, 2, ..., \hat{M}$.

Construct the interpolation matrix $\bar{\boldsymbol{\Phi}}_{\hat{M}\times(M+3)}$ similarly to Step 2.1.

$$\bar{\boldsymbol{\Phi}}_{\hat{M}\times(M+3)} = \bar{\Phi}(\left\|\hat{\mathbf{x}}_j - \mathbf{x}_i\right\|_2, \varepsilon_j) \tag{4}$$

Step 4. The reconstructed pixels, $\widehat{\boldsymbol{G}}_{\hat{M}\times 1}$ is obtained by;

$$\widehat{\boldsymbol{G}}_{\hat{M}\times 1} = \bar{\Phi}_{\hat{M}\times(M+3)}[\boldsymbol{A}]_{(M+3)\times(1)} \tag{5}$$

Step 5. Validating the results by the pre-setup criteria.

4. Numerical experiments and results

The famous Lina image is tackled in this study where the pixels are damaged in the Salt-and-Pepper manner, i.e. the randomly chosen pixels are replaced either by 0 or 255, as shown in Figure 2. Other attempts under this context can also be found in [7, 10-12]. The root mean square error (RMSE), CPU-time and storage, and the mean condition number ($Cond_\delta(-)$) of the interpolation matrices are used as performance criteria. Figure 3 presents two crucial points regarding the effectiveness of each form of GMQ; the accuracy and the sensitivity to shape parameter. It can be seen in this Figure that $\beta = 3/2$ outperforms the others, even the two most popular choices $\beta = -1/2$ and $\beta = 1/2$, in both aspects. Considering the condition number, Table 1 shows, together with the best shape parameter for each GMQ type, that $Cond_\delta(-)$ increases as β increases. The CPU time spent on each simulation, on the other hand, is found not to be significantly different from one another. The quality of the image reconstructed using each GMQ is displayed in Figure 4.

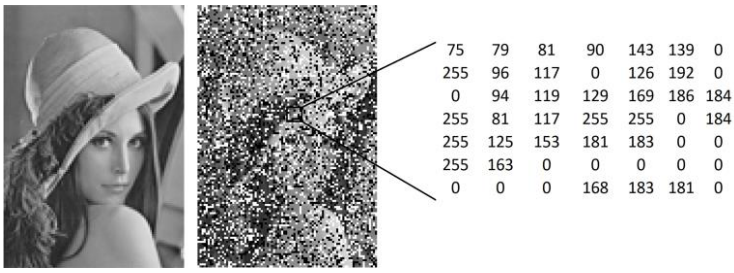

Figure 2. The famous Lena image with the original $88 \times 128 - pixel$ (left), 20%-damaged (middle), and the corresponding pixel values after damaging (right).

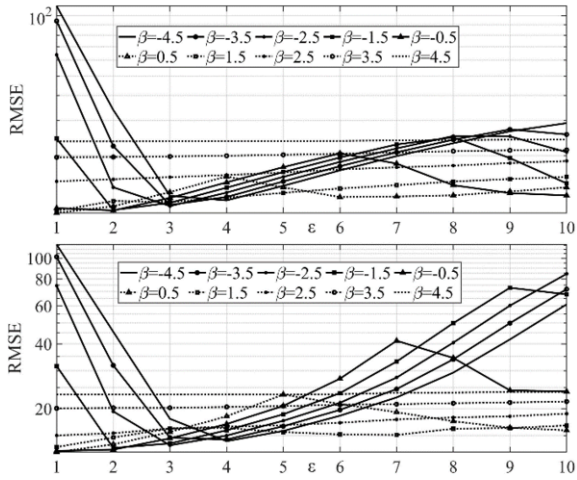

Figure 3. RMSE measured for each form of GMQ with (a) 20%-damage, and (b) 40%-damage, plotted against the shape parameter, ε.

Table 1. Other criteria obtained for each form of GMQ using its best shape parameter.

Criteria	$\beta=-9/2$	$\beta=-7/2$	$\beta=-5/2$	$\beta=-3/2$	$\beta=-1/2$
Best ε	1.00	3.00	3.00	2.00	2.00
RMSE	1.12E+02	1.14E+01	1.12E+01	1.07E+01	1.07E+01
$Cond_{\delta}(-)$	1.39E+00	1.23E+03	5.57E+03	1.09E+03	2.33E+05
CPU-time (s)	8.46E+02	7.20E+02	7.35E+02	6.69E+02	6.67E+02
Criteria	$\beta=1/2$	$\beta=3/2$	$\beta=5/2$	$\beta=7/2$	$\beta=9/2$
Best ε	1.00	1.00	1.00	1.00	1.00
RMSE	1.04E+01	1.06E+01	1.49E+01	1.97E+01	2.36E+01
$Cond_{\delta}(-)$	2.51E+07	1.58E+11	7.67E+14	2.05E+21	1.60E+24
CPU-time (s)	7.63E+02	8.03E+02	6.90E+02	7.80E+02	7.36E+02

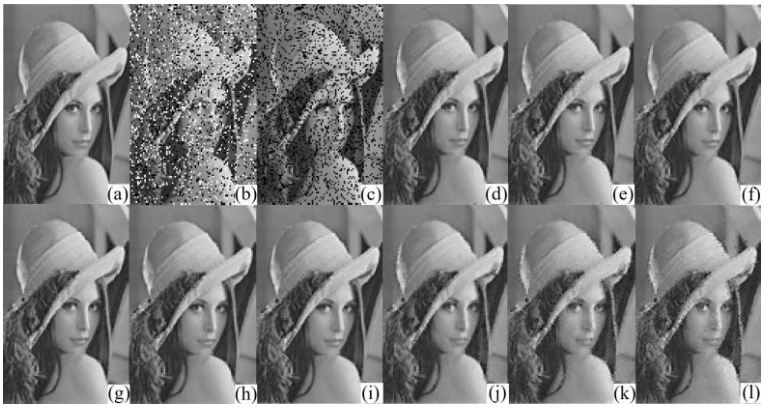

Figure 4. Images under investigation; (a) the original, (b) 20%-damage, (c) reconstructed with $\beta=-9/2$, (d) with $\beta=-7/2$, (e) with $\beta=-5/2$, (f) with $\beta=-3/2$, (g) with $\beta=-1/2$, (h) with $\beta=1/2$, (i) with $\beta=3/2$, (j) with $\beta=5/2$, (k) with $\beta=7/2$, and (l) with $\beta=9/2$.

5. Conclusions

The so-called multiquadric (MQ) radial basis function was numerically studied in more general forms (noted as 'GMQ') in this work. Its applications in image reconstruction tasks were carried out via a structure of a neural network. Ten forms GMQ (differentiated by β) were tested and the corresponding optimal shape parameter for each β was obtained in an 'ad-hoc' manner. This work interestingly reveals that $\beta=3/2$ produces overall best performance over the other forms, even the original, well-known and popular $\beta=-1/2$ and $\beta=-1/2$. Amongst all promising aspects, its ability to stay almost unaffected by the shape ε is most desirable, particularly for more complex applications such as solving partial differential equations (PDEs) and many others, which is the next step of this experiment.

Acknowledgement

This work was supported by (i) Suranaree University of Technology (SUT), (ii) Thailand Science Research Innovation (TSRI), and (iii) National Science, Research and Innovation Fund (NSRF) (NRIIS number 160336).

References

[1] Chen AKCS, Macchion O. A kansa-radial basis function method for elliptic boundary value problems in annular domains. SIAM J. Sci. Comput. 2015;65: 1240-1269.
[2] Chuathong N, Kaennakham S. Numerical solution to coupled burgers' equations by gaussian-based hermite collocation scheme. J Appl Math. Sep. 2018;2018:3416860.
[3] Kansa EJ. Multiquadrics - a scattered data approximation scheme with applications to computational fluid dynamics – I. Comput. Math. Applic.1990;19(8/9):147-161.
[4] Chuathong SKAN. An adaptive inverse multiquadric shape parameter in the reciprocity BEM for solving a nonlinear transient coupled PDE. J Appl Sci. 2017;17:491-501.
[5] Fornberg BP. On choosing a radial basis function and a shape parameter when solving a convective PDE on a sphere. J Comput Phys. 2008;227(5):2758-2780.
[6] Tavaen S, Kaennakham S. A comparison study on shape parameter selection in pattern recognition by radial basis function neural networks. J Physics: Conf Series. 2021;1921(2021);012124.
[7] Natdanai Sriapai PP, Ritthison D, Kaennakham S. On Multiquadric Shape Determining Strategies in Image Reconstruction Applications. 10th International Conference on Mathematical Modeling in Physical Sciences.2021(Accepted for oral presentation).
[8] Sarra MCASA. A numerical study of generalized multiquadric radial basis function interpolation. SIAM Undergraduate Res. Online.2009;2(2):58-70.
[9] Sayan Kaennakham PP, Sriapai N, Tavaen S. Generalized-multiquadric radial basis function neural networks (rbfns) with variable shape parameters for function recovery. Frontiers in Artificial Intelligence and Applications. 2021;340:78-85.
[10] Karel Uhlir VS. Reconstruction of damaged images using Radial Basis Functions. Signal Processing Conference, 2005 13th European, IEEE;2015.p1-4.
[11] Paewpolsong NSP, Tavaen S, Kaennakham S. Image reconstruction by shapefree radial basis function neural networks (RBFNs). J Physics: Conf Series. 2022;2312 (2022);012091.
[12] Perfilieva PVsaaI. Image reconstruction with usage of the F-Transform. Int. JointConf. CISIS'12-ICEUTE'12-SOCO'12. 2013; AISC 189:507-514.